Journal of Sol-Gel Science and Technology (2023) 106:114–120
https://doi.org/10.1007/s10971-023-06052-7

ORIGINAL PAPER: SOL-GEL AND HYBRID MATERIALS FOR DIELECTRIC, ELECTRONIC, MAGNETIC AND FERROELECTRIC APPLICATIONS

Abnormal grain growth and electrical properties of Ba-excessive La-doped $BaTiO_3$ ceramics prepared from nanopowder synthesized by sol-gel method

Hao Zu[1] · Qiuyun Fu[2] · Guohua Cao[3] · Hui Liu[1] · Hui Huang[1] · Liang Yan[1] · Xiaojuan He[1] · Chuanfeng Wang[1]

Received: 15 October 2022 / Accepted: 19 January 2023 / Published online: 7 February 2023

Abstract

Nanopowder is frequently employed in the fabrication of miniaturized multilayer devices due to the advantage of small particle size. In this work, sol-gel method was employed for the synthesis of $Ba_{x\text{-}0.003}La_{0.003}TiO_3$ nanopowders. Abnormal grain growth was observed in the Ba-excessive composition at a relatively low sintering temperature. This result was inconsistent with previous reports that grain growth was suppressed in the Ba-excessive $BaTiO_3$ ceramics. Combining a comparison study, $BaCO_3$, second phase in the powder with $x = 1.03$, was confirmed to be responsible for the abnormal grain growth. Based on the results of SEM, XRD, TG-DTA and electrical properties, it is reasonable to speculate that $BaCO_3$ and oxygen vacancy formed during reduction sintering together triggered the reactive liquid-phase sintering in the $Ba_{x\text{-}0.003}La_{0.003}TiO_3$ ceramics with $x = 1.03$. Thus abnormal grain growth occurred, meanwhile, semiconducting grains was formed.

Graphical Abstract

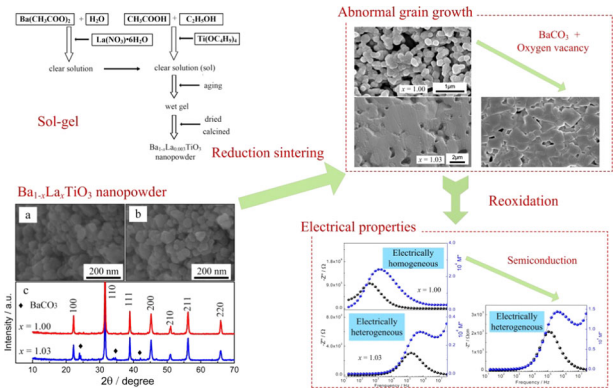

Keywords Sol-gel · $BaTiO_3$ · PTCR · nanopowder · Grain growth · semiconducting grains

✉ Hao Zu
zuh@hfuu.edu.cn

✉ Qiuyun Fu
fuqy@hust.edu.cn

[1] School of Advanced Manufacturing Engineering, Hefei University, Hefei 230601, China

[2] School of Optical and Electronic Information, Huazhong University of Science and Technology, Wuhan 430074, China

[3] Hefei National Laboratory for Physical Sciences at Microscale, University of Science and Technology of China, Hefei 230026, China

Highlights

- Abnormal grain growth was observed in the Ba-excessive La-doped $BaTiO_3$ ceramics prepared from nanopowder synthesized by sol-gel method, when sintered in N_2 atmosphere at a relatively low temperature.
- The $BaCO_3$, as second phase, was found to be responsible for the abnormal grain growth.
- The $BaCO_3$ and oxygen vacancy formed during reduction sintering together triggered the reactive liquid-phase sintering in the $Ba_{x\text{-}0.003}La_{0.003}TiO_3$ ceramics with $x = 1.03$.

1 Introduction

Donor-doped barium titanate ceramics can be an n-type semiconductor and exhibit a positive temperature coefficient of resistivity (PTCR) [1–3]. They have been widely used in electronic circuits as temperature sensors, current limiters, heating devices and so on because of the excellent PTCR effect [4]. Nowadays electronic elements with small volume are urgently needed due to the demands of miniaturized electronic products. Then the PTCR ceramics are fabricated with a multilayer structure to scale down the volume [5]. The grain size of the laminated PTCR ceramics is requested to be very fine to withstand high electric field in the thin layers [6, 7]. Then, nanopowder is frequently employed and critically desired in the fabrication of miniaturized multilayer devices owing to the advantage of small particle size [8]. Thus, it is important to study the microstructural evolution and electrical properties of the PTCR ceramics prepared from nanopowder.

The techniques such as two-step sintering, spark plasma sintering and so on have been confirmed to be effective to suppress grain growth through reducing sintering times or lowering sintering temperatures [8, 9]. However, high-temperature sintering is usually needed for the formation of semiconducting grains in the donor doped $BaTiO_3$ ceramics [10]. Grain coarsening easily appeared during high-temperature sintering, which is not favored in the multilayer PTCR ceramics [10, 11]. Other parameters, such as sintering aids or defects, etc., may also influence the sintering kinetics [12]. For examples, liquid phases were commonly introduced to improve the electrical properties, which could greatly enhance mass transportation and promote the grain growth [13]. Besides, the multilayer PTCR ceramics should be sintered in reducing atmosphere to prevent the oxidation of inner Ni electrodes [14, 15]. The grain growth can be enhanced by the diffusion of oxygen vacancies formed during reduction sintering [12]. Therefore, the grain-size distribution depends crucially on the composition, sintering condition and so on. Although fine-grain PTCR ceramics have been reported by researchers [6, 8, 16], the results have not been full satisfactory to produce fine-grain ceramics, especially with narrow grain-size distribution. Accordingly, it is important to further discover factors that influence the grain growth of PTCR ceramics prepared from nanopowder.

Ba-excessive composition is favored for the fabrication of multilayer PTCR ceramic, because it usually exhibited fine-grain microstructure and high PTCR effect [10]. In the present work, La-doped $BaTiO_3$ nanopowder was synthesized through sol-gel method. The grain growth and electrical properties were studied in the ceramics sintered at a relatively low temperature in N_2 atmosphere. Abnormal grain growth was observed in Ba-excessive ceramics, which was contrary to previous experience. The mechanism for this abnormal phenomenon was further investigated, together with the electrical properties.

2 Experimental details

La-doped $BaTiO_3$ nanopowder with formula $Ba_{x\text{-}0.003}La_{0.003}TiO_3$ ($x = 1.00$ and 1.03) was synthesized by the sol-gel method [3, 16], using $Ba(CH_3COO)_2$ (>99.0%; Sinopharm, China), $La(NO_3)_3{\cdot}6H_2O$ (99.9%; Sinopharm, China) and $Ti(OC_4H_9)_4$ (>98.0%; Sinopharm, China). Details for the synthesis (see Fig. 1) are as follows: $Ti(OC_4H_9)_4$ was diluted in a mixed ethanol-acetic acid solvent to obtain a solution with Ti^{4+} concentration of 1.25 mol/L and stoichiometric amount of $Ba(CH_3COO)_2$ and $La(NO_3)_3{\cdot}6H_2O$ were diluted into deionized water. After 30 min of vigorous stirring at room temperature, two clear solutions were obtained. Then the solution containing Ba^{2+} and La^{3+} was added into the solution containing Ti^{4+} dropwise to avoid the rapid hydrolysis of $Ti(OC_4H_9)_4$. The acquired sol was aged at room temperature for 12 hours and then dried at 90 °C to form gel. The obtained gel was pulverized into powder and calcined at 800 °C in air for 2 hours.

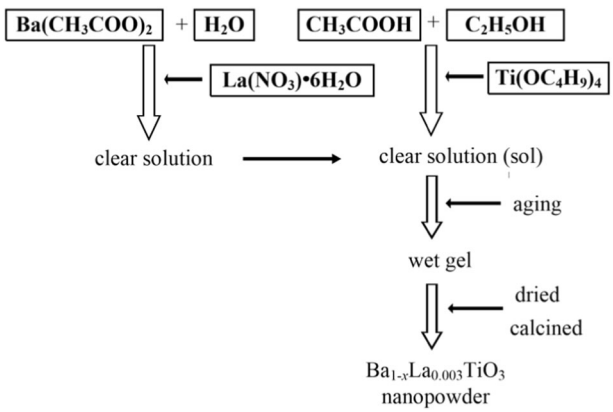

Fig. 1 Scheme of the $Ba_{x\text{-}0.003}La_{0.003}TiO_3$ nanopowder synthesis via sol-gel route

Tape casting method was employed to prepare green pellets as reported previously [17]. The green ceramics were sintered in N_2 atmosphere. The sintering was conducted at temperature range from 1075 to 1150 °C for 2 h. The heating and cooling rates were controlled at 300 °C/h. Then the reduced ceramics were reoxidized at 800 °C for 2 h with a heating rate of 300 °C/h.

Densities of the ceramics were measured by the geometrical method. The X-ray diffraction technique (XRD, XRD-7000s, Shimadzu) was used for the phase composition identification of the raw materials and obtained ceramics. Thermogravimetric and differential thermal analysis (TG-DTA, STA 449F3, Netzsch) were conducted in N_2 atmosphere at a heating rate of 10 °C/min for the raw materials. Scanning electron microscope (SEM, FEI Nova 630) was employed to investigate the microstructures for the raw materials and obtained ceramics. Resistivity-temperature (*R-T*) curves were collected using a computer controlled analyzer at temperatures ranged from room temperature to 250 °C. The PTCR effect was defined as the ratio of the resistivity at 250 °C to that at room temperature (RT). Complex impedance spectroscopy was measured by using a WK6550B impedance analyzer combined with a temperature controller (Huace 650 T, Beijing Huace Testing Instrument Co. Ltd., China).

3 Results and discussions

3.1 Analysis for the synthesized $Ba_{x\text{-}0.003}La_{0.003}TiO_3$ nanopowders

Figure 2 shows the SEM images and XRD patterns of the synthesized powders with a formula of $Ba_{x\text{-}0.003}La_{0.003}TiO_3$ calcined at 800 °C under air atmosphere. From Fig. 2a, b, a similar microstructure can be observed for the two powders and the particle size estimated was about 60 nm. XRD results shown in Fig. 2c suggested that a perovskite structure with a cubic symmetry was formed. Meanwhile, $BaCO_3$ as second phase was observed in the powder with $x = 1.03$, which was also reported in previous studies [18]. It should be noted here that the solution of barium element in $BaTiO_3$ lattice is less than 100 ppm [19, 20], so the excessive barium element in the powder with $x = 1.03$ mainly existed in the form of $BaCO_3$.

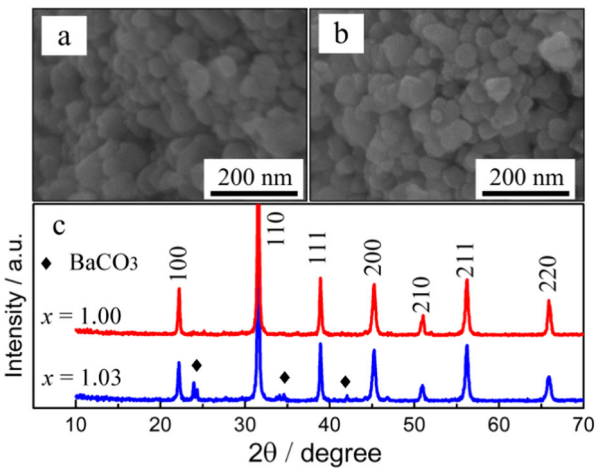

Fig. 2 Characterization for the $Ba_{x\text{-}0.003}La_{0.003}TiO_3$ nanopowders: SEM images of the powder with (**a**) $x = 1.00$ and (**b**) $x = 1.03$. **c** XRD patterns for the synthesized powders

3.2 Microstructural evolution and electrical properties

Figure 3 shows the microstructure of the reduced $Ba_{x\text{-}0.003}La_{0.003}TiO_3$ ceramics sintered at 1100 and 1150 °C, respectively. The grain growth behavior is found to be distinctly different, which was closely dependent on the stoichiometry. At $x = 1.00$, the ceramics exhibited porous microstructures and homogeneous grain-size distributions. The average grain size increased from 60 nm to about 220 and 270 nm after sintered at 1100 and 1150 °C. On the other hand, dense microstructure was observed in the ceramics with $x = 1.03$. The average grain size abnormally increased to about 1.6 and 2.1 μm after sintered at 1100 and 1150 °C, respectively. This result was obviously different from previous reports that grain growth was usually suppressed in Ba-excessive $BaTiO_3$ ceramics prepared by solid-state reaction [10, 21].

Figure 4a shows the influence of sintering temperature on the electrical properties of the $Ba_{x\text{-}0.003}La_{0.003}TiO_3$ ceramics reoxidized at 800 °C. The RT resistivity of the ceramics with $x = 1.03$ was obviously lower than the ones with $x = 1.00$, especially at low sintering temperature. For example, at 1075 °C, the ceramic with $x = 1.00$ was almost insulated and the RT resistance was too high to be measured ($> 10^8$ Ω). However, the RT resistivity became evidently lower and a

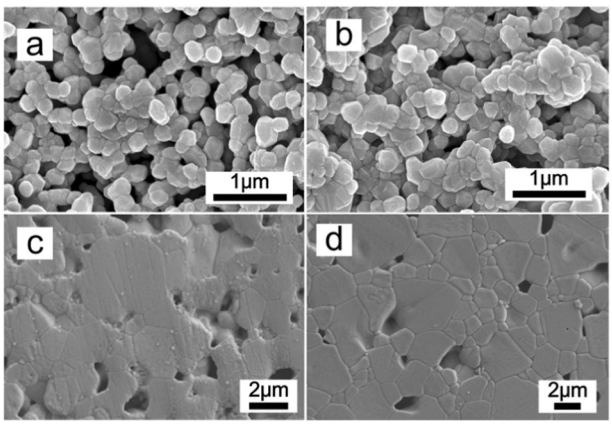

Fig. 3 SEM images of the $Ba_{x\text{-}0.003}La_{0.003}TiO_3$ ceramics sintered at different temperatures: **a** $x = 1.00$, 1100 °C, **b** $x = 1.00$, 1150 °C, **c** $x = 1.03$, 1100 °C and **d** $x = 1.03$, 1150 °C

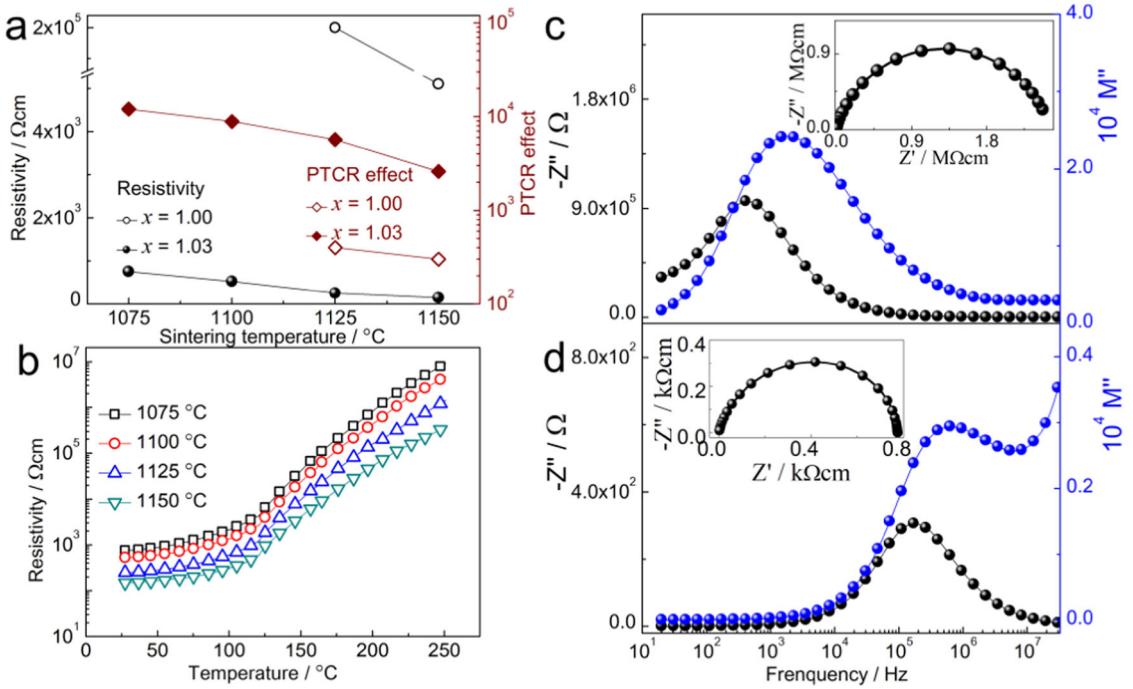

Fig. 4 **a** RT resistivity and PTCR effect for the $Ba_{x\text{-}0.003}La_{0.003}TiO_3$ ceramics sintered at 1075–1150 °C and reoxidized at 800 °C. **b** R-T curves for the ceramics with $x = 1.03$. Impedance analysis for the ceramics with (**c**) $x = 1.00$ and (**d**) $x = 1.03$

value of only 7.5×10^2 Ωcm was obtained at $x = 1.03$. The RT resistivity was able to be further decreased at an elevated sintering temperature and the pronounced PTCR effect could be observed as depicted in Fig. 4b.

Impedance analysis was employed to further investigate the electrical properties and the $Ba_{x\text{-}0.003}La_{0.003}TiO_3$ ceramics sintered at 1075 °C and reoxidized at 800 °C were selected as representatives. Considering that the ceramic with $x = 1.00$ was high resistance, it was then heated to about 500 °C to lower its resistance and then impedance data was collected [22, 23]. In contrast, the ceramic with $x = 1.03$ was low-resistivity and the impedance analysis was conducted at room temperature. Both the ceramics exhibited typical impedance results with a single arc [22], as presented in the insets of Fig. 4c, d.

Note here that the overall resistivity was usually dominated by the grain-boundary resistivity for the PTCR ceramics so that the effect of semiconducting grains on the impedance results sometimes is not easily accessible from the *-Z" vs Z'* plots [23]. The electric modulus, M^*, is a persuasive demonstration to reveal the different electrical properties between the grain and grain boundary [22, 24]. Thus the data from impedance were reprocessed and presented in the electric modulus, M^*, as following equation:

$$M^* = j\omega C_0 Z^* \quad (1)$$

where ω is angular frequency $2\pi f$ and $C_0 = \varepsilon_0 A/l$. ε_0 is the permittivity of free space, 8.854×10^{14} Fcm^{-1}. A is the area of the parallel plate and l is the thickness.

Different imaginary parts of the electric modulus, *M'*, were observed as shown in Fig. 4c, d. Only one peak can be observed in both *-Z"* and *M'* plots for the ceramic with $x = 1.00$ at ~10^3 Hz, which indicated that the bulk was electrically homogeneous and both the grains and grain boundaries were electrically insulated [22, 23]. On the other hand, both *-Z"* and *M'* plots for $x = 1.03$ showed a peak at a relatively low frequency of ~10^5 Hz, which was attributed to the high-resistance grain boundary. Besides, at higher frequency, an increasing incline in the *M'* plot suggested that a peak existed at a frequency above 30 MHz, which originated from the contribution of semiconducting grains [24], as depicted in Fig. 4d. Thus two peaks were expected in *M'* plots, which demonstrated that the ceramic with $x = 1.03$ was an electrically heterogeneous ceramic comprised by semiconducting grains and insulating grain boundaries [22, 25]. Namely, semiconducting grains were able to be formed at a lower sintering temperature and resistant to oxidation in the ceramics with $x = 1.03$.

3.3 Comparison study

Note here that the particle size of the synthesized $Ba_{x\text{-}0.003}La_{0.003}TiO_3$ nanopowder was nearly the same (see Fig. 2), which indicated that the influence of the nano-size particle on the grain growth was approximate. Additionally, the Ba-solubility in $BaTiO_3$ lattice is very limited (< 100 ppm) [19, 20], which was too low to result in the abnormal grain growth as $x = 1.03$. Consequently, the effect of

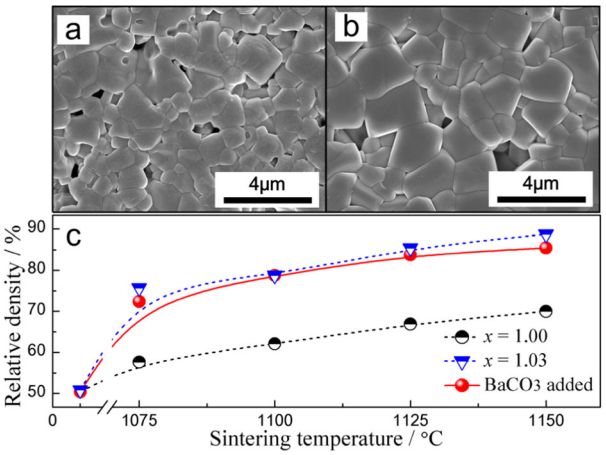

Fig. 5 SEM images of the ceramics with $BaCO_3$ added sintered at different temperature: **a** 1100 °C and **b** 1150 °C. **c** Relative density as a function of sintering temperature

$BaCO_3$, second phase in the powder with $x = 1.03$, was taken into account. In the next experiment, an equivalent amount of $BaCO_3$ (3 mol%), $d_{10} = 0.48$ μm, $d_{50} = 1.36$ μm, $d_{90} = 3.39$ μm, was added directly to the $Ba_{x\text{-}0.003}La_{0.003}TiO_3$ nanopowder with $x = 1.00$ to exclude the Ba-solubility but maintain the second phase $BaCO_3$. The grains grew up again to about 1.2 and 2.1μm and the densification was enhanced as $BaCO_3$ was added into the powder with $x = 1.00$, as shown in Fig. 5. Both the average grain size and relative density became close to the ceramics with $x = 1.03$.

Furthermore, compared with the ceramics with $x = 1.00$, the electrical properties were also changed by the addition of $BaCO_3$, especially at low sintering temperature, as shown in Fig. 6. Complex impedance was conducted to analysis the effect of $BaCO_3$ on the electrical property of grains and grain boundaries shown in Fig. 6a, b. It can be found that one arc was observed in the -Z'' vs Z' plot, but two peaks were also expected in the electric modulus, M'', plot for the ceramics sintered at 1075 °C and reoxidized at 800 °C, similar to the ceramic with $x = 1.03$ (see Fig. 4d). This result suggested that an electrically heterogeneous microstructure was able to be formed at a lower sintering temperature as $BaCO_3$ was induced. Due to the formation of semiconducting grains, the insulating property disappeared, meanwhile, the RT resistivity decreased to about 5.3×10^3 Ωcm and PTCR effect was observed as presented in Fig. 6c, d. Based on the above narratives, it can be concluded that $BaCO_3$ should be responsible for the abnormal grain growth and formation of semiconducting grains at a relative low sintering temperature.

3.4 Analysis of grain growth and electrical properties

TG-DTA was employed to analyze the thermal behavior for the powder with $x = 1.00$ and 1.03 under N_2 atmosphere as shown in Fig. 7. Clearly, different weight loss and endothermic events occurred between the two powders. As $x = 1.00$, the smooth TG-DTA curves (Fig. 7a) indicated that the composition was relatively thermostable under N_2 atmosphere. However, two distinct endothermic peaks (peak A and B) were observed in the DTA curve as $x = 1.03$. Meanwhile, a weight loss occurred together with the peak A at temperature above ~800 °C shown in Fig. 7b. To further clarify this endothermic event (peak A), green pellets were calcined at 700 and 900 °C in N_2 atmosphere for 2 h, which were then pulverized into powder for phase identification. The peak of $BaCO_3$ disappeared, meanwhile, the peak of Ba_2TiO_4 was observed as shown in Fig. 8. Combining the results of TG-DTA and XRD, it can speculate that the endothermic peak A corresponds to a chemical reaction, which was also reported pervious [26, 27]:

$$BaTiO_3 + BaCO_3 \rightarrow Ba_2TiO_4 + CO_2(g) \quad (2)$$

Note here that the $BaCO_3$ has a low melting point of only 811 °C, but Valant et al. found that the grain growth could not be promoted by $BaCO_3$ only. Because the melted $BaCO_3$ reacted rapidly with the $BaTiO_3$ matrix and then was consumed when the sintering temperature was elevated up to the melting point as depicted in Eq. 2 [26]. However, oxygen vacancies $\left(V_O^{\bullet\bullet}\right)$ can be easily created in $BaTiO_3$ lattice during the reduction sintering through the equation below [14]

$$2O_O^{\times} \rightarrow 2V_O^{\bullet\bullet} + 4e' + O_2(g) \quad (3)$$

The lattice-diffusion coefficient is proportional to the concentration of $V_O^{\bullet\bullet}$, as a result, the sintering was kinetically enhanced by the diffusion of $V_O^{\bullet\bullet}$ [26]. A similar low-temperature sintering, named reactive liquid-phase sintering, has been achieved by many authors through the incorporation of Li^+ into $BaTiO_3$ lattice resulting in the formation of $V_O^{\bullet\bullet}$ [27, 28]. Namely, the $BaCO_3$ and the $V_O^{\bullet\bullet}$ together triggered the reactive liquid-phase sintering leading to the abnormal grain growth in the $Ba_{x\text{-}0.003}La_{0.003}TiO_3$ ceramics with $x = 1.03$ at a relatively low temperature as shown in Fig. 3.

On the other hand, accompanying with the first peak, another endothermic peak B was presented in the DTA curve shown in Fig. 7b, which was not observed in the $BaTiO_3$-$BaCO_3$ system reported previously. According to the phase diagram for BaO-TiO_2 system, the Ba_2TiO_4 phase was thermostable in $BaTiO_3$ matrix indicating that no reaction occurred between $BaTiO_3$ and Ba_2TiO_4 [19]. Considering that no weight loss was observed or too small to be detected in the TG curve in Fig. 7b, the second peak (peak B) was possibly induced by a variation of crystal structure. Combing with the above results that semiconducting grains could be formed after sintered at a relatively low temperature as $x = 1.03$ (see Fig. 6), it can speculate that an insulating phase

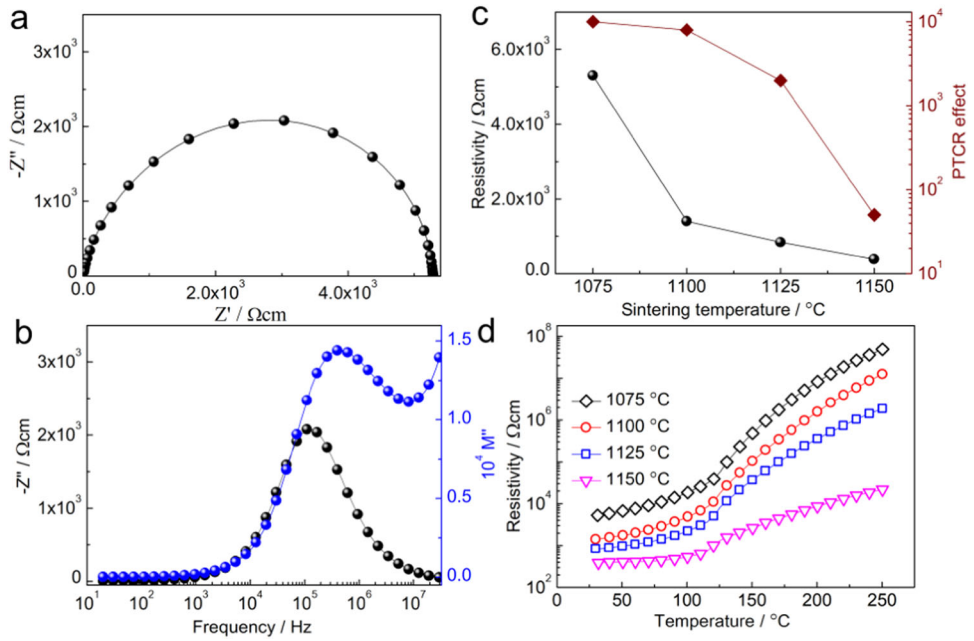

Fig. 6 **a** Impedance analysis, **b** impedance, -*Z*'', and modulus, *M*'', plot at room temperature, **c** RT resistivity and PTCR effect and **d** R-T curves for the ceramics with $BaCO_3$ added

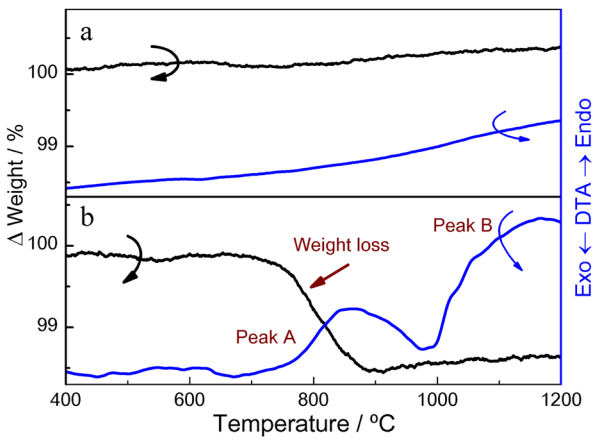

Fig. 7 TG-DTA curves for the $Ba_{x\text{-}0.003}La_{0.003}TiO_3$ ceramics conducted in N_2 atmosphere: **a** $x = 1.00$ and **b** $x = 1.03$

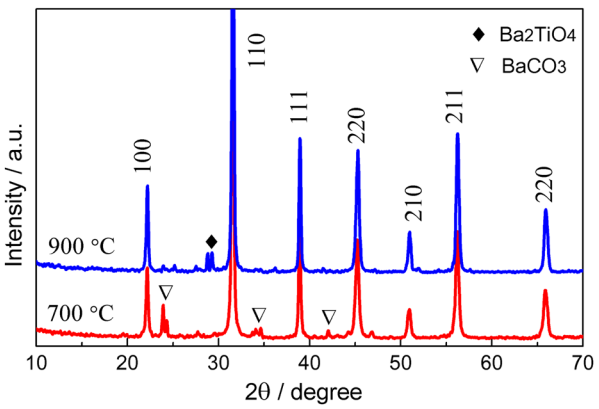

Fig. 8 XRD patterns for the nanopowder with $x = 1.03$ calcined at 700 and 900 °C in N_2 atmosphere

$(Ba_{1-x}La_x^{\bullet}Ti_{1-x/4}^{\times}V_{Tix/4}^{''''}O_3)$ might be transformed into a semiconducting phase $(Ba_{1-x}La_x^{\bullet}Ti_{1-x}^{\times}Ti_x'O_3)$, which can be described by a following simplified equation [29]:

$$Ba_{1-x}La_x^{\bullet}Ti_{1-x/4}^{\times}V_{Tix/4}^{''''}O_3 \rightarrow Ba_{1-x}La_x^{\bullet}Ti_{1-x}^{\times}Ti_x'O_3 + Ba_2TiO_4 + O_2(g) \quad (4)$$

This result was well consistent with previous studies that semiconducting grains were usually formed along with the abnormal grain growth [11], which was also observed in the $Ba_{x\text{-}0.003}La_{0.003}TiO_3$ ceramics with $x = 1.03$ shown in Fig. 3. Noted here that a trace of oxygen could be released during this process, but the concentration was too low to be detected by TG analysis as reported previously [30].

4 Conclusion

Semiconducting La-doped barium titanate ceramics were fabricated by reduction-reoxidation method from nanopowders synthesized by sol-gel method. Excessive barium element in the nanopowder was mainly existed in the form of $BaCO_3$, which was found to be able to introduce two endothermic peaks in the DTA curve conducted in N_2 atmosphere. Combining with the results of thermogravimetric, X-ray diffraction, electron microscopy and electrical measurements, it can speculate that the reactive liquid-phase sintering was triggered in the Ba-excessive La-doped ceramics sintered in N_2 atmosphere. Then abnormal grain growth occurred and the insulating grains transformed into semiconducting grains during this process.

Acknowledgements This work was supported by the National Natural Science Foundation of China (grant No. 12004368), the China Postdoctoral Science Foundation (grant No. 2020M671859), the Anhui Provincial Natural Science Foundation (Grant No. 2108085QE198), the University Natural Science Research Project of Anhui Province (Grant No. KJ2019A0840, KJ2020A0652, gxyq2022071 and 2021kcszsfkc360) and the Talent Research Foundation of Hefei University (Grant No. 18-19RC36). The authors acknowledge the assistance by the Analytical and Testing Center of Huazhong University of Science and Technology.

Compliance with ethical standards

Conflict of interest The authors declare no competing interests.

References

1. Rowlands W, Vaidhyanathan B (2018) Additive manufacturing of barium titanate based ceramic heaters with positive temperature coefficient of resistance (PTCR). J Eur Ceram Soc 39:3475–3483
2. Leng S, Cheng H, Zhang R, Gao C, Li Z (2021) Electrical properties of La-Mn-codoped $BaTiO_3$-$(Bi_{0.5}Na_{0.5})TiO_3$ lead-free PTCR ceramics. Ceram Int 47:30963–30968
3. Ianculescu AC, Vasilescu CA, Crisan M, Raileanu M, Vasile BS, Calugaru M, Crisan D, Dragan N, Curecheriu L, Mitoseriu L (2015) Formation mechanism and characteristics of lanthanum-doped $BaTiO_3$ powders and ceramics prepared by the sol-gel process. Mater Charact 106:195–207
4. Zu H, Chen T, Gao C, Gao C, Fu Q, Zhou D, Hu Y, Zheng Z, Luo W (2017) Abnormal reoxidation effects in Ba-excess La-doped $BaTiO_3$ ceramics prepared by the reduction-reoxidation method. J Am Ceram Soc 100:2958–2964
5. Yan L, Fu Q, Zhou D, Wang M, Zheng Z, Luo W, Wang G (2019) Enhanced electrical properties of $BaTiO_3$-based thermosensitive ceramics for multilayer chip thermistors applications by addition of $(Bi_{0.5}Na_{0.5})TiO_3$. Ceram Int 45:19113–19119
6. Brutchey RL, Cheng G, Gu Q, Morse DE (2008) Positive Temperature Coefficient of Resistivity in Donor-Doped $BaTiO_3$ Ceramics derived from Nanocrystals synthesized at Low Temperature. Adv Mater 20:1029–1033
7. Zhao Q, Gong H, Wang X, Chen I-W, Li L (2016) Superior Reliability Via Two-Step Sintering Barium Titanate Ceramics. J Am Ceram Soc 99:191–197
8. Gao C, Fu Q, Zhou D, Zu H, Chen T, Xue F, Hu Y, Zheng Z, Luo W (2017) Nanocrystalline semiconducting donor-doped $BaTiO_3$ ceramics for laminated PTC thermistor. J Eur Ceram Soc 37:1523–1528
9. Luan W, Gao L, Kawaoka H, Sekino T, Niihara K (2004) Fabrication and characteristics of fine-grained $BaTiO_3$ ceramics by spark plasma sintering. Ceram Int 30:405–410
10. Niimi H, Mihara K, Sakabe Y, Kuwabara M (2007) Influence of Ba/Ti ratio on the positive temperature coefficient of resistivity characteristics of Ca-doped semiconducting $BaTiO_3$ fired in reducing atmosphere and reoxidized in air. J Am Ceram Soc 90:1817–1821
11. Drofenik M, Makovec D, Zajc I, Langhammer HT (2002) Anomalous grain growth in donor-doped barium titanate with excess barium oxide. J Am Ceram Soc 85:653–660
12. Levi RD, Tsur Y (2005) The effect of oxygen vacancies in the early stages of $BaTiO_3$ nanopowder sintering. Adv Mater 17:1606–1608
13. Wang X, Chan HL-W, Choy C-L (2004) Positive temperature coefficient of resistivity effect in niobium-doped barium titanate ceramics obtained at low sintering temperature. J Eur Ceram Soc 24:1227–1231
14. Zu H, Fu Q, Gao C, Chen T, Zhou D, Hu Y, Zheng Z, Luo W (2018) Effects of $BaCO_3$ addition on the microstructure and electrical properties of La-doped barium titanate ceramics prepared by reduction-reoxidation method. J Eur Ceram Soc 38:113–118
15. Niimi H, Mihara K, Sakabe Y, Kuwabara M (2007) Preparation of Multilayer Semiconducting $BaTiO_3$ Ceramics Co-Fired with Ni Inner Electrodes. Jpn J Appl Phys 46:6715–6718
16. Niesz K, Ould-Ely T, Tsukamoto H, Morse DE (2011) Engineering grain size and electrical properties of donor-doped barium titanate ceramics. Ceram Int 37:303–311
17. Zhou D, Zhao D, Fu Q, Hu Y, Jian G, Cheng X, Shen X (2012) Particle sizes effects on electrical properties and densification of laminated $Ba_{1.002}La_{0.003}TiO_3$ ceramics. Ceram Int 39(3):2457–2462
18. Aghayan M, Zak AK, Behdani M, Hashim AM (2014) Sol-gel combustion synthesis of Zr-doped $BaTiO_3$ nanopowders and ceramics: Dielectric and ferroelectric studies. Ceram Int 40:16141–16146
19. Lee S, Randall CA, Liu ZK (2007) Modified phase diagram for the barium oxide–titanium dioxide system for the ferroelectric barium titanate. J Am Ceram Soc 90:2589–2594
20. Hu YH, Harmer MP, Smyth DM (1985) Solubility of BaO in $BaTiO_3$. J Am Ceram Soc 68:372–376
21. Leng S, Li G, Zheng L, Cheng L, Zeng J (2011) Influences of Ba/Ti Ratios on the Positive Temperature Coefficient of Resistivity Effect of Y-Doped $BaTiO_3$-$(Bi_{1/2}Na_{1/2})TiO_3$ Ceramics. J Am Ceram Soc 94:1340–1342
22. Irvine JTS, Sinclair DC, West AR (1990) Electroceramics: characterization by impedance spectroscopy. Adv mater 2:132–138
23. Beltrán H, Cordoncillo E, Escribano P, Sinclair DC, West AR (2004) Insulating Properties of Lanthanum-Doped $BaTiO_3$ Ceramics Prepared by Low-Temperature Synthesis. J Am Ceram Soc 87:2132–2134
24. Morrison FD, Sinclair DC, West AR (2001) Characterization of lanthanum-doped barium titanate ceramics using impedance spectroscopy. J Am Ceram Soc 84:531–538
25. Yoon SH, Kim H (2002) Space charge segregation during the cooling process and its effect on the grain boundary impedance in Nb-doped $BaTiO_3$. J Eur Ceram Soc 22:689–696
26. Valant M, Suvorov D, Pullar RC, Sarma K, Alford NM (2006) A mechanism for low-temperature sintering. J Eur Ceram Soc 26:2777–2783
27. Valant M, Suvorov D (2004) Low-Temperature Sintering of $(Ba_{0.6}Sr_{0.4})TiO_3$. J Am Ceram Soc 87:1222–1226
28. Wang SF, Yang TC, Huebner W, Chu JP (2000) Liquid-phase sintering and chemical inhomogeneity in the $BaTiO_3$-$BaCO_3$-LiF system. J Mater Res 15:407–416
29. Makovec D, Drofenik M (2000) Microstructural changes during the reduction/reoxidation process in donor-doped $BaTiO_3$ ceramics. J Am Ceram Soc 83:2593–2599
30. Drofenik M, Popović A, Irmančnik L, Kolar D, Kraševec V (1982) Release of oxygen during the sintering of doped $BaTiO_3$ ceramics. J Am Ceram Soc 65:C-203-C-204